Predicting the Effects of Deep Brain Stimulation with Diffusion Tensor Based Electric Field Models*

Christopher R. Butson[1], Scott E. Cooper[2], Jaimie M. Henderson[3], and Cameron C. McIntyre[1,2]

[1] Department of Biomedical Engineering, Cleveland Clinic Foundation, Cleveland, OH
butsonc@ccf.org
[2] Center for Neurological Restoration, Cleveland Clinic Foundation, Cleveland, OH
[3] Department of Neurosurgery, Stanford School of Medicine, Stanford, CA

Abstract. Deep brain stimulation (DBS) is an established therapy for the treatment of movement disorders, and has shown promising results for the treatment of a wide range of other neurological disorders. However, little is known about the mechanism of action of DBS or the volume of brain tissue affected by stimulation. We have developed methods that use anatomical and diffusion tensor MRI (DTI) data to predict the volume of tissue activated (VTA) during DBS. We co-register the imaging data with detailed finite element models of the brain and stimulating electrode to enable anatomically and electrically accurate predictions of the spread of stimulation. One critical component of the model is the DTI tensor field that is used to represent the 3-dimensionally anisotropic and inhomogeneous tissue conductivity. With this system we are able to fuse structural and functional information to study a relevant clinical problem: DBS of the subthalamic nucleus for the treatment of Parkinsons disease (PD). Our results show that inclusion of the tensor field in our model caused significant differences in the size and shape of the VTA when compared to a homogeneous, isotropic tissue volume. The magnitude of these differences was proportional to the stimulation voltage. Our model predictions are validated by comparing spread of predicted activation to observed effects of oculomotor nerve stimulation in a PD patient. In turn, the 3D tissue electrical properties of the brain play an important role in regulating the spread of neural activation generated by DBS.

1 Introduction

Deep brain stimulation (DBS) is an effective, proven therapy for the treatment of Parkinson's Disease (PD), essential tremor and dystonia. The realization that

* The authors would like to thank Ashu Chaturvedi, Barbara Wolgamuth, and Christopher Maks for their technical assistance on this project. This work was supported by grants from the American Parkinson Disease Association, the Ohio Biomedical Research and Technology Transfer Partnership, and the National Institutes of Health (NS-50449 & NS-52042).

R. Larsen, M. Nielsen, and J. Sporring (Eds.): MICCAI 2006, LNCS 4191, pp. 429–437, 2006.

high frequency DBS generates clinical benefits analogous to those achieved by surgical lesioning has transformed the use of functional neurosurgery for the treatment of movement disorders [1,2,3]. Thalamic DBS for intractable tremor has virtually replaced ablative lesions of the thalamus [4]. And, DBS of the subthalamic nucleus (STN) or globus pallidus internus has largely replaced pallidotomy in the treatment of the cardinal motor features of PD (resting tremor, rigidity, bradykinesia) [5]. In addition, multiple pilot studies have begun to examine the utility of DBS for dystonia, epilepsy, obsessive-compulsive disorder, and depression. However, the clinical successes of DBS are tempered by our limited understanding of the effects of DBS on the nervous system, and the therapeutic mechanisms of DBS remain unknown [6].

The fundamental purpose of DBS is to modulate neural activity with extracellular electric fields, but the technology necessary to accurately predict and visualize the neural response to DBS has not been previously available. In turn, the current state-of-the-art in pre-operative targeting strategies and post-operative parameter selection processes do not take into account the influence of the electric field generated by the DBS electrode on the surrounding neural structures. DBS systems provide thousands of possible stimulation configurations, resulting in great flexibility in customization of therapy for individual patients, but at the expense of time-consuming clinical evaluation to determine therapeutic stimulation settings [7]. As a result, DBS patient management is primarily based on trial-and-error as opposed to quantitative understanding. To address these limitations, we have developed techniques to predict the volume of tissue activated (VTA) during DBS [8]. We have previously shown that the electrode-tissue interface and the encapsulation layer surrounding the electrode can cause substantial differences in the VTA volume. The electrode-tissue interface interacts with the time course of the stimulation waveform such that longer pulse widths are more strongly attenuated [9]. Similarly, high electrode impedances are correlated with greater electrode encapsulation, which also reduces the VTA volume [10]. However, these previous studies were conducted using a homogeneous, isotropic tissue medium which is useful for parameterizing the effects of DBS but does not take into account the complex properties of neural tissue. In this paper we explore the effects of 3-dimensional tissue electrical properties on the VTA generated by DBS. Specifically, tissue conductivity is extracted from diffusion tensor MRI (DTI) data and coregistered with pre-operative and post-operative anatomical MRIs. With this method we are able to create a realistic volume conductor for use in a finite element field model of the brain [11,12]. Until now there have been few methods available to predict or visualize the effects of DBS on individual patient brains. The innovation of this paper is to predict the volume of tissue activated during stimulation using quantitative forward field models. This type of model is potentially useful to the EEG/MEG community because it provides a forward field solution to brain dynamics that can be used to validate the inverse models often used for localizing neural activity. The results presented in this paper are the first clinically validated, patient-specific models of DBS for predicting neural activation.

2 Methods

The DBS system consists of a quadripolar electrode lead, an implantable pulse generator (IPG) and an extension wire connecting the two (Figure 1). The electrode lead is implanted during stereotactic surgery; the work presented in this paper focuses on STN DBS. Each electrode contact is 1.27 mm diameter and 1.5 mm height, and electrodes are separated by either a 1.5 mm (3387 model) or 0.5 mm (3389 model) insulation gap. The DBS system can be operated in multi-polar or monopolar configurations with any combination of anodes and cathodes; during monopolar stimulation the return electrode is the IPG case. Typical settings for monopolar STN DBS are -3 V, 90 μsec pulse width and 130 Hz. For therapeutic stimulation settings, symptomatic relief of PD symptoms is normally achieved within a few seconds.

We have developed techniques to predict the spread of activation during DBS by combining several imaging methods into a single coherent framework (Figure 1). First, a pre-operative T1 MRI (collected on a Siemans 1.5T scanner) was segmented using SNT software (Surgical Navigation Technologies, a division of Medtronic, Minneapolis, MN, USA) based on the non-linear warping techniques of [13] to produce closed surfaces for several basal ganglia nuclei: STN, thalamus, globus pallidus, putamen, caudate and accumbens (only STN and thalamus are shown in the figures). Second, a post-operative T1 MRI was used to determine the position of the electrode. Electrode localization was performed by isosurfacing progressively smaller values of the electrode artifact until the surface converged onto a volume containing the 4 electrode contacts. The pre-operative and post-operative MR volumes were then co-registered with fractional anisotropy values from a DTI atlas brain using Analyze 6.0 (AnalyzeDirect, Lenexa, KS, USA). The DTI atlas brain is explained in detail in [14]. Briefly, images were acquired on a 1.5-T Philips Gyroscan MR using single-shot echo-planar imaging sequences. The imaging matrix was 112 x 112 with a field of view of 246 x 246 mm. Transverse sections of 2.2 mm thickness were acquired for a total of 55 slices. Diffusion weighting was encoded along 30 independent orientations, and the b value was $700 mm^2/sec$. Imaging was repeated six times to enhance the signal to noise ratio. The six independent elements of the 3 x 3 diffusion tensor were calculated for each pixel by using a multivariate linear fitting method.

Accurate representation of the stimulating electrodes and the surrounding electric field is made possible with two techniques: multiresolution meshes and dynamic interpolation. Finite element methods are used to model geometric features and boundary conditions for which analytical solutions do not exist. A finite element model of the DBS electrode and surrounding tissue medium was constructed using FEMLAB 3.1 (Comsol Inc., Burlington, MA, USA). Multi-resolution meshes allow node density to be highest where the electric field is changing the fastest. The second technique, dynamic interpolation, allows the electrode to be easily moved to arbitrary positions and orientations within the brain volume without repeating the computationally costly and time-consuming step of creating a new mesh. With these methods, DTI tensors are dynamically interpolated onto the finite element mesh, an operation that takes 10-15 seconds for approximately

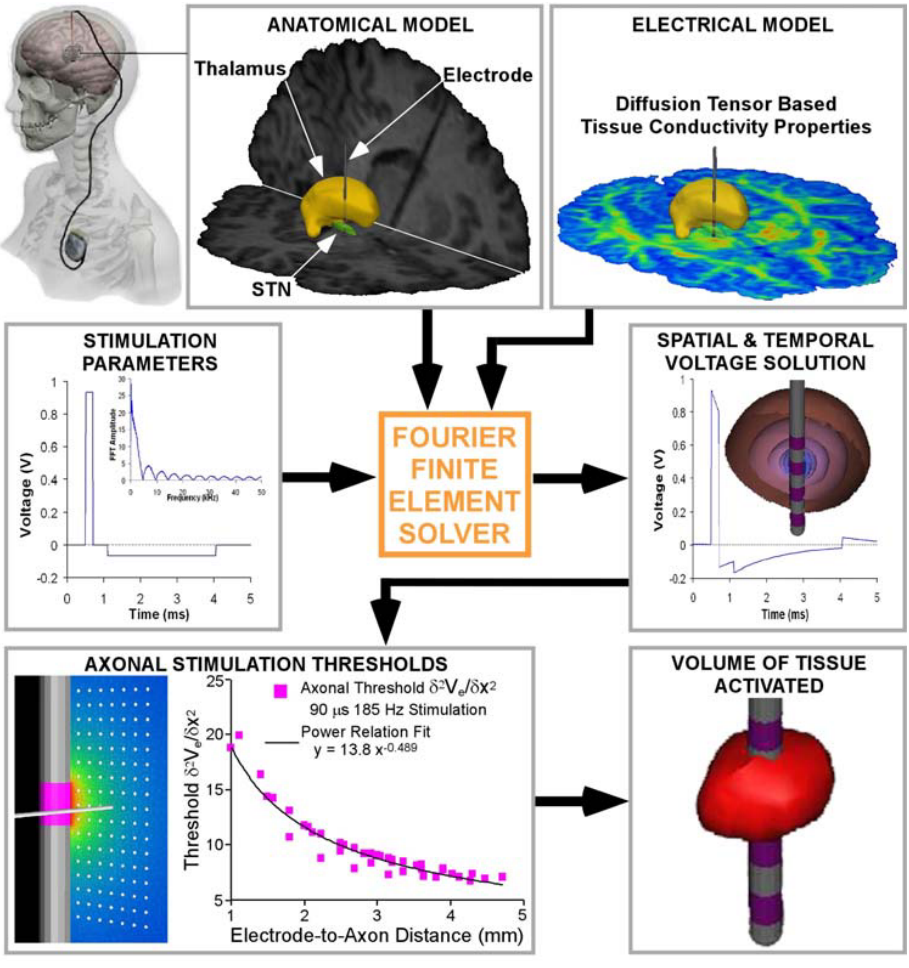

Fig. 1. Methods. The DBS system is implanted as shown. Pre-operative, post-operative and DTI MRIs are coregistered, the stimulation waveform is applied to the electrode, and the system is solved using the Fourier FEM solver. The resulting time- and space-dependent voltages are used to calculated activating function thresholds for fibers of passage, and the VTA is determined using these thresholds.

215,000 nodes and 1.9e6 DTI tensors on an 8-processor SGI Prism with 32 GB RAM. Lastly, boundary conditions for the stimulation parameters at each electrode contact are dynamically interpolated onto the brain mesh.

The conductivity tensor is directly solved for at each voxel using a simple linear transform [15]: $\sigma = (\sigma_e/d_e)D$, where σ_e is the effective extracellular conductivity, d_e is the effective extracellular diffusivity and D is the diffusion tensor. The ratio of (σ_e/d_e) has been determined from experimental and empirical data to be ˜0.7 (S - s)/mm2 [12,15]. This value is then scaled to match the electrode impedance recorded from the IPG of the given patient.

VTAs are calculated with stimulation prediction techniques that integrate finite element based electric field solutions with multi-compartment cable models of myelinated axons [16,17,11]. The Poisson equation is solved with a Fourier FEM solver [9] to determine voltage as a function of time and space within the tissue medium:

$$\nabla \cdot \sigma \nabla \Phi = -I \tag{1}$$

where Φ is voltage, I represents injected current and σ is a complex stiffness matrix that includes the DTI conductivities and the reactive components of the electrode-tissue interface. The voltage solution is subsequently interpolated onto the model neurons to determine stimulation thresholds for action potential generation. Activating function values are then defined from the second difference of the voltage solution ($\delta^2 V_e / \delta x^2$) and used to provide a spatial map for VTA prediction. Simulations and visualization were conducted using BioPSE [18].

3 Effects of DTI-Based Tissue Conductivity on Bioelectric Field Modeling

We found that the use of DTI-based tissue conductivities caused substantial differences in the activation of anatomical targets when compared to a homogeneous, isotropic tissue medium (Figure 2a). First, the VTAs calculated using

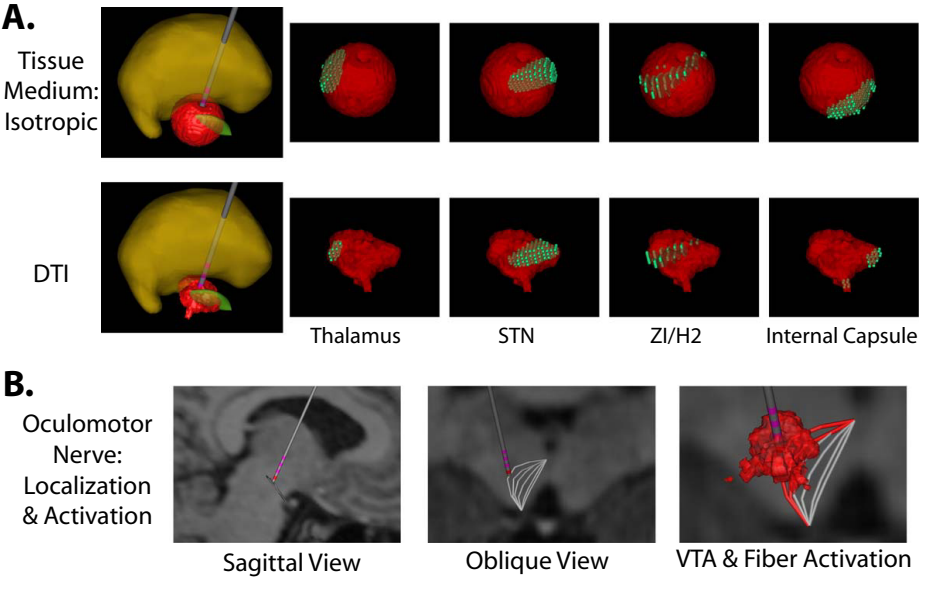

Fig. 2. Results. A) VTAs are compared between isotropic and DTI-based tissue mediums, illustrating the difference in the size and shape of the VTAs (leftmost images) as well as the differential activation of thalamus, STN, ZI/H2 and internal capsule (images at right, activation of subvolumes shown in light green). B) These results are validated by comparing predicted thresholds to those observed during activation of the oculomotor nerve in a PD patient (VTA at -6 V shown, fibers in red are activated).

the two different methods have very different shapes. As expected, the VTA generated with the isotropic medium is nearly spherical. Alternately, the VTA generated using the DTI conductivities is non-spherical and asymmetric. The differences in shape are due to the 3D tissue properties and cannot be explained by a change in the mean conductivity of the isotropic volume. Second, we observed that the VTAs generated under the two conditions caused differential activation of the thalamus, STN, zona incerta and fields of Forel (ZI/H2), and internal capsule. These structures have direct relevance for STN DBS: activation of the thalamus and internal capsule is believed to be correlated with side effects, while activation of STN and ZI/H2 is correlated with therapeutic effects. The magnitude of the difference was dependent on both the shape of the VTA and its total volume, which is directly proportional to the stimulation parameters (voltage and pulse width).

4 Activation of Oculomotor Nerve in Parkinson's Disease Patient

We compared model predictions to patient outcomes by looking for activation of discrete target structures with clear clinical signs. One such structure that is relevant to STN DBS is the oculomotor nerve (cranial nerve III), which is attractive for several reasons: it is visible on MR (Figure 2b); it has well defined borders; stimulation of this nerve manifests itself with clear clinical signs (ocular deviations ipsilateral to the side of the brain being stimulated). We conducted these experiments on a 51 year old male PD patient with bilateral DBS electrodes implanted in both STNs (Medtronic 3387 electrodes and Soletra IPGs). The patient received informed consent to participate in the study and the protocol was approved by the Institutional Review Board at the Cleveland Clinic. The oculomotor nerve on the right side of the patient brain was localized on a parasagittal slice along a line from the point it exits the midbrain to midway through the superior colliculus. The position of the fibers within this oblique plane was determined with a 3D atlas [19]. While PD patients are normally stimulated at therapeutic frequencies over 100 Hz, in these experiments the patient was stimulated at 2 Hz, which has the advantage of producing neither paresthesias nor fused muscle contractions. Hence, muscle twitches are directly observable by the clinician and in some cases can be sensed by the patient. The patient was stimulated with the electrode on the right side of the brain at 2 Hz, 120 μsec pulse width while voltage magnitude was increased from 0 V to -7 V in -1 V increments. Thresholds for activation of the oculomotor nerve during monopolar stimulation of contact 0 (the most distal contact) were detected by an observer at -4 V, and were sensed by the patient at -6 V. Corresponding simulations indicate good agreement with our experimental results (Figure 2b). With the DTI volume, the VTA was just touching the border of the oculomotor fibers at -4 V. At higher voltages, progressively more of the fibers were activated as indicated by intersection of the VTA with the fiber bundles. In contrast, the threshold for activation with the isotropic medium was -1 V.

5 Discussion

Existing DBS systems were adapted from cardiac pacing technology ~20 years ago. The original design of the Medtronic 3387/3389 DBS electrode was hindered by limited knowledge of the neural stimulation objectives of the device. Recent advances in neural engineering design tools, such as the computer modeling techniques used in this study, were not available when DBS was invented. In addition, the therapeutic mechanisms of action remain an issue of controversy [6]. Until direct neurophysiological relationships can be determined between the stimulation and therapeutic benefit, true engineering optimization of DBS devices will remain difficult. However, the neurostimulation prediction tools used in this study provide a new technology platform that can be used to advance three important areas in DBS research. First, patient-specific models of DBS can be used to advance our scientific understanding of the effects of DBS [11,16]. Development of correlations between VTA spread into various anatomical nuclei under therapeutic and non-therapeutic stimulation conditions provides the basis for definition of an anatomical and electrical target for the stimulation. Second, patient-specific models of DBS can be used to improve clinical adjustment of the stimulation parameters [20]. Development of clinician-friendly software incorporating 3D visualization graphics of the MRI data, anatomical nuclei, DBS electrode, and VTA as a function of the stimulation parameters provides the basis for decreasing the level of intuitive skill necessary to perform clinical DBS parameter selection. Third, anatomically and electrically accurate models of DBS can be used for the development of novel electrode designs that optimize the shape of the VTA to maximize therapeutic outcome [8]. Development of theoretically optimal electrode designs for a given stimulation target area in the brain and neurological disorder has the potential to minimize side effects generated by the stimulation and maximize therapeutic benefit from DBS.

This paper demonstrates results from a clinically validated, patient-specific model of DBS. The gold standard for this type of experimental model would use microelectrode recordings in addition to the physiological results presented in the paper. However, microelectrode recordings can only be made very briefly and in areas close to the electrode target due to patient safety considerations. Nonetheless, the results of this study show that when 3D tissue conductivities derived from DTI data are incorporated into our model of neurostimulation they substantially impact the VTA. Only with the DTI-based conductivities were we able to achieve good agreement between our model predictions and clinical results. In addition, we have previously shown that electrode capacitance and electrode encapsulation also play important roles in defining the VTA. In turn, attempts to make quantitative correlations between stimulation parameters and behavioral measurements on a patient-by-patient basis should explicitly account for the effects of electrode capacitance, electrode impedance, and the 3D tissue electrical properties of the tissue medium surrounding the DBS electrode.

References

1. Benabid, A.L., Pollak, P., Louveau, A., Henry, S., de Rougemont, J.: Combined (thalamotomy and stimulation) stereotactic surgery of the vim thalamic nucleus for bilateral parkinson disease. Appl Neurophysiol **50** (1987) 344–6
2. Benabid, A., Pollak, P., Gervason, C., Hoffmann, D., Gao, D., Hommel, M., Perret, J., de Rougemont, J.: Long-term suppression of tremor by chronic stimulation of the ventral intermediate thalamic nucleus. Lancet **337** (1991) 403–406 Reprint Status: In File.
3. Gross, R.E., Lozano, A.M.: Advances in neurostimulation for movement disorders. Neurol Res **22** (2000) 247–58
4. Benabid, A.L., Pollak, P., Gao, D., Hoffmann, D., Limousin, P., Gay, E., Payen, I., Benazzouz, A.: Chronic electrical stimulation of the ventralis intermedius nucleus of the thalamus as a treatment of movement disorders. J Neurosurg **84** (1996) 203–14
5. Kumar, R., Lang, A.E., Rodriguez-Oroz, M.C., Lozano, A.M., Limousin, P., Pollak, P., Benabid, A.L., Guridi, J., Ramos, E., van der Linden, C., Vandewalle, A., Caemaert, J., Lannoo, E., van den Abbeele, D., Vingerhoets, G., Wolters, M., Obeso, J.A.: Deep brain stimulation of the globus pallidus pars interna in advanced parkinson's disease. Neurology. **55** (2000) S34–9
6. McIntyre, C.C., Savasta, M., Kerkerian-Le Goff, L., Vitek, J.L.: Uncovering the mechanism(s) of action of deep brain stimulation: activation, inhibition, or both. Clin Neurophysiol **115** (2004) 1239–48
7. Obeso, J., Olanow, C., Rodriguez-Oroz, M., Krack, P., Kumar, R., Lang, A.: Deep-brain stimulation of the subthalamic nucleus or the pars interna of the globus pallidus in parkinson's disease. N Engl J Med **345** (2001) 956–63
8. Butson, C., McIntyre, C.C.: Role of electrode design on the volume of tissue activated during deep brain stimulation. J Neural Eng **3** (2006) 1–8
9. Butson, C.R., McIntyre, C.C.: Tissue and electrode capacitance reduce neural activation volumes during deep brain stimulation. Clin Neurophysiol **116** (2005) 2490–500
10. Butson, C.R., Maks, C.B., McIntyre, C.C.: Sources and effects of electrode impedance during deep brain stimulation. Clin Neurophysiol **117** (2006) 447–54
11. McIntyre, C.C., Mori, S., Sherman, D.L., Thakor, N.V., Vitek, J.L.: Electric field and stimulating influence generated by deep brain stimulation of the subthalamic nucleus. Clin Neurophysiol **115** (2004) 589–95
12. Tuch, D.S., Wedeen, V.J., Dale, A.M., George, J.S., Belliveau, J.W.: Conductivity tensor mapping of the human brain using diffusion tensor mri. Proc Natl Acad Sci U S A **98** (2001) 11697–701
13. Christensen, G.E., Joshi, S.C., Miller, M.I.: Volumetric transformation of brain anatomy. IEEE Trans Med Imaging **16** (1997) 864–77 0278-0062 (Print) Journal Article.
14. Wakana, S., Jiang, H., Nagae-Poetscher, L.M., van Zijl, P.C., Mori, S.: Fiber tract-based atlas of human white matter anatomy. Radiology **230** (2004) 77–87 0033-8419 Journal Article.
15. Haueisen, J., Tuch, D.S., Ramon, C., Schimpf, P.H., Wedeen, V.J., George, J.S., Belliveau, J.W.: The influence of brain tissue anisotropy on human eeg and meg. Neuroimage **15** (2002) 159–66

16. Butson, C., Hall, J., Henderson, J., McIntyre, C.: Patient-specific models of deep brain stimulation: 3d visualization of anatomy, electrode and volume of activation as a function of the stimulation parameters. In: Society for Neuroscience. Volume 30:1011.11. (2004)
17. McIntyre, C.C., Richardson, A.G., Grill, W.M.: Modeling the excitability of mammalian nerve fibers: influence of afterpotentials on the recovery cycle. J Neurophysiol **87** (2002) 995–1006
18. BioPSE: Scientific Computing and Imaging Institute (SCI),http://software.sci.utah.edu/biopse.html, 2002.
19. Haines, D.E.: Neuroanatomy : an atlas of structures, sections, and systems. 5th edn. Lippincott Williams & Wilkins, Philadelphia (2000)
20. Butson, C., Maks, C., Cooper, S.E., Henderson, J.M., McIntyre, C.C.: Deep brain stimulation interactive visualization system. In: Society for Neuroscience. Volume 898.7., Washington, D.C. (2005)